Excerpt from the Proceedings of the 2011 COMSOL Conference in Stuttgart

Study of Gas Dynamics in the Heat-Accumulation Stoves

P. Scotton[1,] *, D. Rossi[1,] **
[1]University of Padova, Department of Geosciences, Gradenigo street n. 6, Italy 35131

[1,] *paolo.scotton@unipd.it, [1,] **danielerossi74@gmail.com

Abstract: The research aims to clarify some aspects of the gas hydrodynamics within the twisted conduct present in the heat accumulation stoves (ceramic-refractory stoves). The high temperature combustion products flow in the twisted conduct releasing heat to the refractory. The stored heat is returned to the environment as radiant heat. During this process may occur transition from laminar to turbulent motion in the conduct. Both Comsol laminar and k-ε turbulent models have been used in case of straight and curved pipes with circular, square and rectangular cross sections, at different Reynolds numbers, in case of smooth wall. Comsol Navier-Stokes model properly simulates fluxes at low Reynolds numbers. k-ε and k-ε at low Reynolds numbers models properly simulate the motion at high Reynolds numbers. In the transition zone, 3000< Re <7000, the solution of the k-ε at low Reynolds numbers appears distant from the literature results and strongly dependent on the computing grid.

Keywords: laminar flow, turbulent flow, heat transfer, dynamics of combustion gases.

1. Introduction

The research regards a particular kind of heat accumulation stoves made of ceramic and refractory. They are a traditional heating element of the European Alpine regions, whose history began in the fifteenth century. They consist of a combustion chamber, where woody material is burned, followed by a twisted conduct where the high temperature products of combustion flow, giving off heat to the refractory. Due to the heat transfer along the pipe the kinematic viscosity decreases, by increasing the Reynolds number and causing transition from laminar to turbulent motion. Moreover the continuous changes of direction imposed by the curves, cause local contractions and expansions of the flux and, consequently, energy losses which are difficult to evaluate.

The stored heat is returned slowly to the environment in the form of radiant heat from the ceramic tiles of the external surface.

The way the heat exchange happens depends mainly on gas flow conditions (laminar or turbulent) and on conduct physical properties (roughness of the internal surface of the conduct), as well as the mass of refractory material and its geometric arrangement.

The attempt to describe these phenomena is the goal of the present research, in order to provide increased awareness in the design process of these technological elements, which are strongly affected by the uncertainties above described. We expect to obtain important consequences also in terms of energy saving and pollution control (optimizing the combustion process and control over the production of fine particles).

Figure 1: Left: historical “Sfruz” heat accumulation stove, located in the Buonconsiglio Castle in Trento, Italy. Right: view of a project design of modern stoves, where can see combustion chamber and twisted conduct.

2. Physical considerations

The accumulation stoves represent a technological system for space heating through radiant heat. The heat is generated in a combustion chamber that burns a determined amount of woody material at high temperatures and in a short period of time. The heat is accumulated in the refractory material with high density and high heat capacity, arranged around the combustion chamber and around the conduct of the combustion gases, and is returned to the environment as radiant heat from the outer surface of the stove at lower temperatures and for a much larger duration than the generation time (Figure 2).

In the traditional accumulation stove the motion of the gases produced by the combustion is caused by the pressure difference between the local atmospheric pressure and the air pressure in the entrance zone of the air necessary to the combustion. That pressure difference is caused by the density variation between the cold atmospheric air and the hot air in the chimney (Figure 3), as well as the height of the chimney. It can be estimated as follows:

$$P_A - P_B = (\rho_a - \rho_f) \cdot g \cdot \Delta H \qquad \textbf{Eq. 01}$$

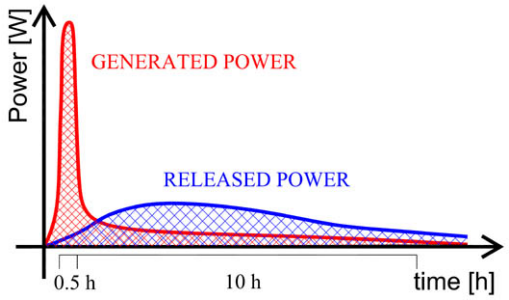

Figure 2: Scheme of the thermal attenuation generated by an accumulation stove. High power for a low duration of the thermal power produced in the combustion chamber, in red. In blue the low power for a long duration of the thermal power released by the external surface of the stove.

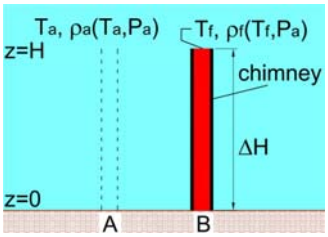

Figure 3: The driving force of the combustion gases is due to the difference between the density of the air in the atmosphere and the density of the gases inside the chimney.

So, the driving power is a function of the elevation, of the air temperature, of the atmospheric pressure, of the gases temperature and of the height of the Chimney. In Figure 4 an idea of the values in Pa of the driving force is given. It has been evaluated considering the standard atmosphere, an air temperature of 5 °C and a height of the chimney of 5 m.

At constant air temperature and chimney height the driving force increases strongly with the temperature of combustion gases and decreases with the elevation where the stove is located. To identify the basic hydrodynamic characteristics of the gases motion, some numerical evaluations were carried out in permanent motion conditions.

It has been hypothesized that the stove is located at an altitude of 500 m asl, that the outside air temperature is equal to 5°C, that the chimney height is equal to 5 m and that the total length of the conduct (chimney height plus the length of the twisted conduct) is 10 m.

The diameter of the pipe has been set equal to 0.18 m, 0.25 m and 0.35 m. The relative roughness of the pipe, e/D was set equal to 0.002. The temperature of the combustion gases was kept constant at 10°C, 100°C and 500°C. These may represent the average temperature of the gases at different moments of functioning of the stove.

It is also assumed the presence of 5 90° bends and 4 180° bends. The ratio, Rc/D, between the curvature radius and the diameter of the pipe was set equal to 0.5 and 1. The energy dissipation due to the bends were evaluated according Idel'cik, 1960.

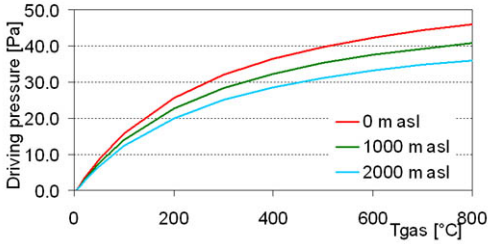

Figure 4: Driving pressure of gases in the twisted conduct inside the stove and in the chimney.

Figure 5 shows how gases velocity increases with increasing temperature and with increasing radius of curvature of the bends and remains essentially unchanged with increasing area of the pipe.

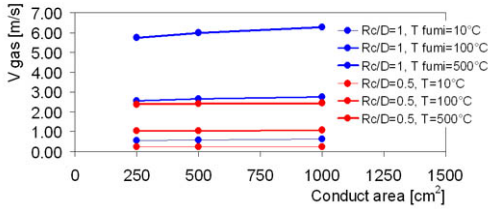

Figure 5: The mean velocity of gases as a function of the pipe area, gases temperature and geometry of curves.

Figure 6 shows how the mass discharge of combustion gases increases with increasing area of the pipe, gases temperature and radius of curvature of the pipe.

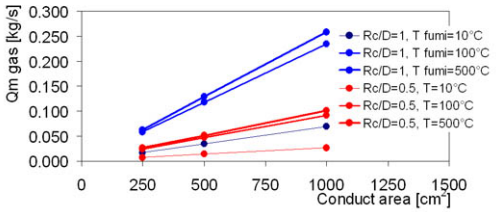

Figure 6: Mass discharge in the pipe as a function of the area of the pipe, gases temperature and geometry of curves.

Figure 7 shows the behaviour of the Reynolds number with temperature of the combustion gases. The evaluations were carried out taking into account the variation of the density and viscosity of gases at different temperatures:

$$\rho_{gas}(T = 10°C) / \rho_{gas}(T = 500°C) \cong 2.7;$$
$$\nu_{gas}(T = 10°C) / \nu_{gas}(T = 500°C) \cong 0.136.$$

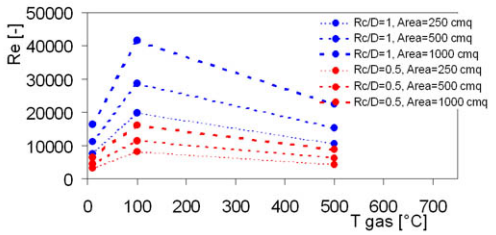

Figure 7: Reynolds number in the pipe as a function of gas temperature, of the area of the pipe and of the geometry of curves.

The Reynolds number takes values for which the motion is in transition conditions between laminar and turbulent flow. Under these conditions the estimate of dissipation, due mainly to the curves, is particularly delicate.

The simple considerations described above show that it is necessary to increase the quality of the analysis of the problem in order to obtain design capabilities closer to the physical phenomenon.

3. Numerical Model

In the first phase of the research Comsol Multiphysics has been used to simulate the hydrodynamics of combusted gases. Straight and curved conducts of different sections have been considered (round, square and rectangular). Both laminar, turbulent at low Reynolds numbers and turbulent flow model have been tested.

3.1 Straight pipe

The 'uniform' motion inside a straight pipe can be modeled using a 2D axial symmetry. In the simulations we have varied the Reynolds number from 1000 to 100.000.

For Reynolds between 1000 and 3000 Navier-Stokes model has been used, whereas for Reynolds larger than 3000 the k-ε turbulent model and the k-ε model at low Reynolds numbers have been used.

For all models the boundary conditions in the fluid domain were:

- velocity at the inlets. Only for turbulent models, the turbulent length scale ($L_T = 0.7 \cdot D$) has been set, in order to take into account boundary layer effects;
- pressure at the outlets;
- the contact condition at the wall, was imposed for laminar motion ($U = 0$), while for turbulent flows a logarithmic wall function was used. This condition provides for the velocity a no penetration condition into the viscous sublayer ($U \cdot \hat{n} = 0$); a homogeneous Neumann condition for the turbulent kinetic energy, $\hat{n} \cdot \nabla k = 0$, and the condition $\varepsilon = u_\tau^3 / k\delta_W$ for the dissipation rate of turbulence energy. In the turbulent flows, the steep gradients close to the walls do not permit to solve the flow variables. For this reason in k-ε turbulent model has been assumed that the computational domain begin at a distance δ_W from the wall. The distance δ_W is computed so that δ_W^+ becomes 11,06. At the end of each simulation was checked that δ_W^+ was 11,06 on most of the walls. When the k-ε at low Reynolds numbers model has been used, the wall boundary condition was a "no slip" condition, which means that the velocity and the turbulent kinetic energy are zero ($U = 0$, $k = 0$). This because that model evaluated the

physical variables also in the viscous sublayer till the wall. In this case, for dissipation rate of turbulence energy, the boundary condition reads $\varepsilon = 2k\mu / l_W^2 \rho$. At the end of each simulation was checked that the dimensionless distance to cell center l_C^* was near unity on most of the walls.

3.1.1 Mesh and Solver

It must be said that the choice of the kind of mesh depends on the shape of the computational domain (for instance with or without sharp curves), as well as on flow conditions (laminar or turbulent).

For solving our problems we have used all kind of available meshes.

For straight pipes (2D axial simmetry), the laminar flow has been solved using a structured mesh, called "mapped mesh" in COMSOL. The turbulent flows have been solved, both with the k-ε turbulent model and the k-ε at low Reynolds number, using an unstructured mesh, called " free triangular" in COMSOL (Table 1).

Model	Space Dim.	DOF (10^6)	Type Mesh used for
N. – S.	2D Axial	0,250	mapped
k-ε		0,590	free triangular
k-ε LR		1,300	free triangular

Table 1: Space dimension, Degree of Freedom of matrices system and type of mesh used for the diferent models in case of straight pipe.

3.2 Curved pipe

The changes of direction in the pipes have been made with the introduction of elbows and sharp curves. The contraction of the flow, starting from the inner edge of the curve, and the successive expansion generate a loss of energy. The energy drop, due to the curve, can be expressed with the equation:

$$\Delta E = \xi \frac{V^2}{2g} \qquad \textbf{Eq. 02}$$

where ξ has to be estimated. Besides, at the curves, secondary current develop in the cross section.

A literature case has been simulated (H. Meckel, 1976, in Ghetti 1987): a 25° curved pipe with radius of curvature equal to 26 m and pipe diameter of 2 m (Figure 8). The fluid was water with mean velocity equal to 3.63 m/s.

Other simulations have been made of a double sharp curve in a pipe with a diameter of 160 mm, where the fluid was air (Figure 9). Results of numerical simulations have been compared with laboratory experiments with Reynolds number ranging from 2500 up to 35000.

Figure 8: Curved pipe (25°, radius of curvature 26 m): pipe diameter equal to 2 m, mean velocity equal to 3.63 m/s.

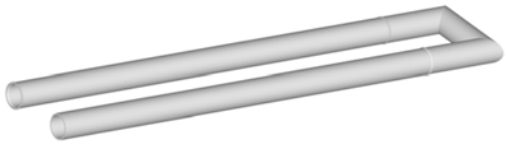

Figure 9: A double sharp curve: pipe diameter equal to 160 mm; Reynolds number from 2500 up to 35000.

Due to the secondary currents it has not been possible to simplify the model with one geometric symmetry. The 3D geometric space dimension has been used.

For Reynolds numbers until values of 3000 Navier-Stokes model was used. For Reynolds larger than 3000 the k-ε turbulent model has been used.

The boundary conditions were the same as in the case of a straight pipe (see 3.1 Straight pipe).

3.2.1 Mesh and Solver

For curved pipes (space dimension 3D), unstructured meshes have been used, called "free tetrahedral" in COMSOL. In addition, a boundary layer mesh has been used. The thickness of the first layer was estimate respecting the rule:

$$h_{FL} \leq 2 \cdot \delta_W \qquad \textbf{Eq. 03}$$

In the first case, 25° curved pipe, the motion regime is turbulent, fully developed, and so the k-ε model has been used.

For the simulations of the double sharp curve with increasing Reynolds numbers, from 2500 up to 35000, Navier-Stokes model when Reynolds was less than 3000, and k-ε turbulent model with Reynolds higher than 3000 have been used (Table 2).

25° CURVED PIPE			
Model	Space Dim.	DOF (10^6)	Type Mesh used for
k-ε	3D	0,710	free tetrahedral + boundary layer
DOUBLE SHARP CURVE			
Model	Space Dim.	DOF (10^6)	Type Mesh used for
NS	3D	0,350	free tetrahedral
k-ε	3D	1,200	free tetrahedral + boundary layer

Table 2: Space dimension, Degree of Freedom of matrices system and type of mesh used for the diferent models in case of curved pipe.

4. Experimental Results

4.1 Straight pipe

In the case of laminar flow, numerical cross-sectional velocity distribution has been compared with velocity laminar law (Eq. 4) whereas, for turbulent flow, the comparison has been made with velocity defect law (Eq. 5). From the simulations the resistance number has been calculated and compare with the expression f=64/Re, in case of laminar flow, and with Colebrook-White expression, in case of turbulent flow.

$$u = -\frac{\gamma \cdot j}{4 \cdot \mu} \cdot \left(r^2 - R^2\right) \qquad \textbf{Eq. 04}$$

$$\frac{u - u_m}{u_*} = \frac{1}{k}\left[2\sqrt{r/R} + \ln\frac{1-\sqrt{r/R}}{1+\sqrt{r/R}}\right] \qquad \textbf{Eq. 05}$$

In Figure 10 numerical cross-sectional velocity distribution has been compared with laminar and defect law.

In Figure 11 numerical values of the resistance number are showed, together with the Moody diagram, obtained from the application of Navier-Stokes model, k-ε at low Reynolds numbers turbulent model and k- ε turbulent model, in case of straight pipes. The agreement in laminar conditions with Navier-Stokes model is quite good. The same can be said when using k- ε turbulent model with Reynolds number larger than 10.000, if the walls of the pipe can be considered smooth. The application of the k- ε at low Reynolds numbers turbulent model has proved to be rather delicate and significanty dependent on the generation of a "good" mesh. In the figure are reported the best results obtained.

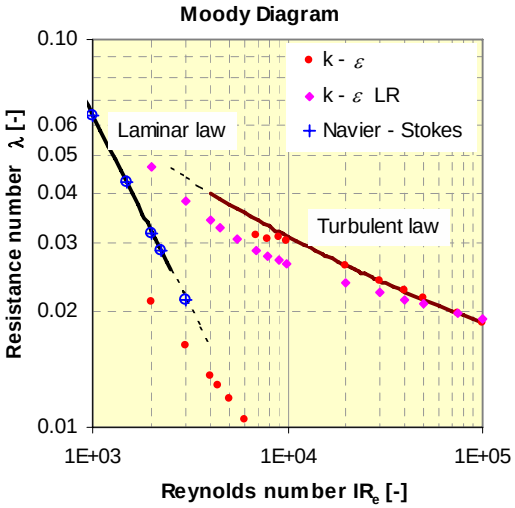

Figure 11: Numerical Resistance number, obtained with Comsol, showed together with the Moody diagram: behaviour of different models (Navier-Stokes, k-ε and k-ε at low Reynolds number).

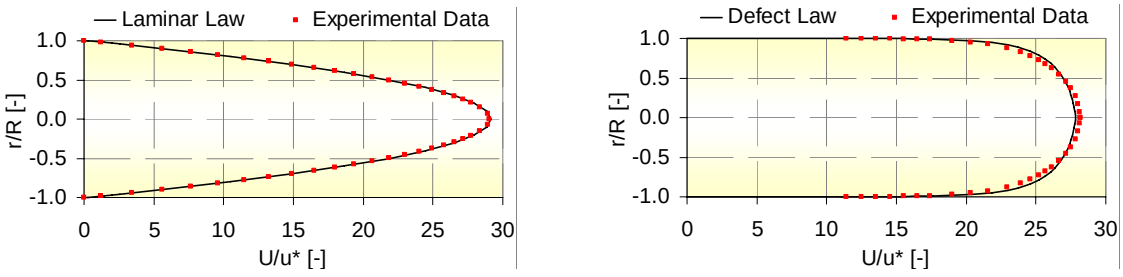

Figure 10: Comparison between numerical results and literature data of velocity distribution in a straight, circular cross section pipe. On the left:Re = 1.700; on the right: Re = 500.000.

4.2 Curved pipe

Case 1: 25° curved pipe.

In Figure 12 is reported the velocity distribution at a section of a circular pipe located at a distance of 11.7 diameters after a curve of 25° (H. Meckel, 1976, in Ghetti 1987; pipe diameter equal to 2 m, mean velocity equal to 3.63 m/s), in case of fully developed turbulent motion.The k-ε turbulent model describes properly the generations of secondary currents that modify drastically the motion field. The differences compared to experimental data may also be due to the surface properties of the pipe, always considered smooth by the Comsol model.

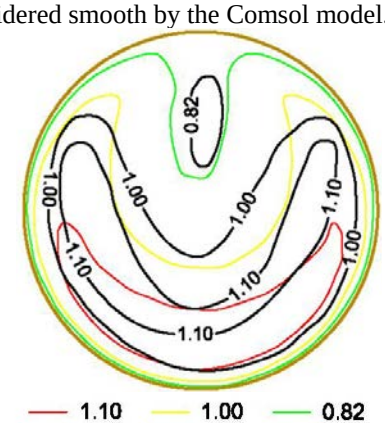

Figure 12: Comparison between experimental data (black lines in the figure; H. Meckel 1976) and numerical data of velocity distribution, downstream a curve in fully developed turbulence conditions.

Case 2: double sharp curve.

In Figure 13 the energy loss coefficient ξ (Eq. 02) due to a double sharp curve have been reported. The values calculated with the numerical simulations are compared with the values obtained on a physical model by Barberi s.r.l. (Barberi s.r.l., 2011).

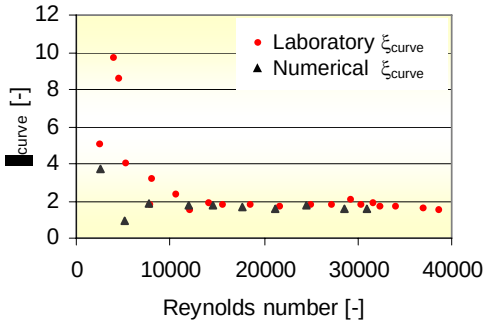

Figure 13: Estimation of coefficient ξ (Eq. 02) for a double sharp curve. Comparison between numerical data and laboratory experimental data (Barberi srl, 2011).

The numerical estimation and the physical model approximation appear in a quite good agreement when Reynolds number is larger than 10.000. At low Reynolds numbers differences are much larger.

5. Conclusions

The use of numerical methods available in Comsol (vers. 4.0–4.2) to the solution of the complicated equations of turbulence has shown some significant limitations for the current research. These include the inability to consider the rough walls in the k-ε and in the k- ε at low Reynolds numbers turbulent model and the strong dependence of the results from computing grid when using the k- ε turbulent model at low Reynolds number.

The research is currently continuing, in situations where the methods are considered reliable, with the introduction of the equations describing the heat exchange between the different elements of the heat accumulation stoves.

6. References

1. S. Torii, Laminarization of strongly heated gas flows in a circular tube, *JSME International Journal*, **Vol. 33**, page 538 – 547 (1990).
2. J. Nagano, A new low-Reynolds-Number One-Equation Model of Turbulence, *Flow, Turbulence and Combustion*, **Vol. 63**, page 135 – 151 (1999).
3. R. J. Garde, *Turbulent Flow*. New Age International, (2010).
4. A. Ghetti, *Idraulica*. Ed. Cortina, Padova (1987).
5. Barberi s.r.l., 2001, Personal comm..
6. Comsol manuals.

7. Acknowledgements

The research has been financed by the Trentino (Italy) Provincial law n. 6, 1999, call 2008.